Research Article | Vol. 27, No. 26 / 23 December 2019 / Optics Express 37516
Optics EXPRESS

Low-loss pedestal Ta_2O_5 nonlinear optical waveguides

JULIÁN H. SIERRA,[1] RICARDO C. RANGEL,[1] RICARDO E. SAMAD,[2] NILSON DIAS VIEIRA JR.,[2] MARCO I. ALAYO,[1] AND DANIEL O. CARVALHO[3,*]

[1] *Polytechnic School, University of São Paulo (USP), São Paulo SP 05508-010, Brazil*
[2] *Center for Lasers and Applications, IPEN-CNEN/SP, São Paulo SP 05508-000, Brazil*
[3] *Currently with the Telecommunications Department, São Paulo State University (UNESP), São João da Boa Vista SP 13876-750, Brazil*
[*] *daniel.orquiza@unesp.br*

Abstract: In this work, we investigate a pedestal tantalum oxide (Ta_2O_5) material platform for integrated nonlinear optics (NLO). In order to achieve low propagation losses with this material, pedestal waveguides with Ta_2O_5 cores were designed. The nonlinear refractive index n_2 of this new platform was obtained by measuring the amount of spectral broadening due to self-phase modulation (SPM) of 23 fs optical pulses at 785 nm propagating through the waveguides. In this manner, a nonlinear index of $(5.8 \pm 2.0) \times 10^{-19}$ m^2W^{-1} was found for this material, which is in good agreement with values reported in related works where strip waveguides were used for a similar purpose. Furthermore, due to the pedestal configuration, propagation losses as low as 1.6 $dB{\cdot}cm^{-1}$ for narrow waveguides and 0.1 $dB{\cdot}cm^{-1}$ for large waveguides were obtained. Finite element method (FEM) mode analysis was performed to calculate the mode characteristics, as well as the effective areas of the waveguides. The high nonlinear and linear refractive indices, wide bandgap and low propagation losses make this platform ideal for applications extending from the visible into the mid-IR regions of the optical spectrum. Due the large gap, Ta_2O_5 should have low two photon absorption at the near-IR as well.

1. Introduction

Integrated nonlinear optics is an exciting area that in the last decade has demonstrated a breadth of miniaturized devices with potential to have great impact in many fields such as optical communications and optical interconnects for electronics, to cite a few [1–3]. The first highly successful integrated platform ever demonstrated was based on silicon on insulator (SOI). Devices for wide-band optical amplification, wavelength conversion as well as multiple wavelength coherent optical sources could benefit from integration with electronics and lead the way to smaller, more efficient devices built for the future networks [4–6]. The most attractive feature of integrated photonics is that, due to the possibility of having high refractive indices contrast, smaller modal areas and larger nonlinear parameters can be achieved. This means that shorter devices could be used with similar efficiencies, which theoretically makes devices such as optical parametric amplifiers (OPAs) feasible. It is well known that the great lengths needed to implement OPAs in fibers translate into large stimulated brilloin scattering (SBS), which needs to be suppressed for proper amplification. Miniaturized devices were potentially the perfect solution for this problem. Soon other platforms started to be explored because silicon, although having a very high nonlinear response, suffers from high linear and non-linear losses.

New platforms, such as silicon nitride (Si_3N_4) and hydex, among others, have been proposed in the recent past, and each has its positive and negative characteristics [7,8]. Most of these platforms allow for a much wider band of operation than silicon, and have been used in the fabrication of devices for demonstrating frequency comb generation, wavelength conversion,

#380625 https://doi.org/10.1364/OE.27.037516
Journal © 2019 Received 17 Oct 2019; revised 16 Nov 2019; accepted 26 Nov 2019; published 11 Dec 2019

Optics EXPRESS

parametric amplification, among others [9–11]. Si_3N_4 requires high temperatures for its LPCVD deposition. These high temperatures, along with the high compressive mechanical stress, lead to a cumbersome fabrication process in order to avoid cracking and structural damages to the devices. Hydex, on the other hand, is a proprietary material and has a somewhat lower refractive index that translates into lower mode confinement and thus, less pronounced nonlinear effects.

This work is a first step towards developing a new platform for Nonlinear photonics based on pedestal Ta_2O_5 waveguides. Its relatively high refractive index (n = 2.07), which is comparable to that of silicon nitride, leads to waveguides with high mode confinement and a large nonlinear coefficient (γ). A high refractive index can also translate into more flexibility for dispersion engineering in these materials. Tantalum oxide films, used here to obtain the core of the pedestal waveguides, can be made by sputtering at low temperature and are CMOS-compatible. Ta_2O_5 has a bandgap of 4.3 eV and good transparency in the near and mid-infrared, as well as a negligible two-photon absorption (TPA) coefficient at near-infrared wavelengths.

The development of a waveguide fabrication process requires some engineering with respect to the lithographic process, as well as etching recipes that are key to obtaining small scattering losses. If this engineering is not done properly, waveguides with overly high propagation losses can be obtained. This is specially true for waveguides in which the core is composed of transition metal oxides. For this reason, we have proposed a new way to access the nonlinear property of unexplored materials [12]. This method involves using pedestal waveguides, in which the material is deposited on top of a pedestal that is previously defined in the lower cladding layer. In this way there is no etching of the material that composes the waveguide's core. The pedestal process used in this work has the advantage of leading to waveguides with losses that are much smaller than that of rib or strip waveguides. Therefore, the use of the pedestal process is an integral part of the platform proposed here, as opposed to previous works [13,14].

The nonlinear index of Ta_2O_5 was measured through self phase modulation (SPM) induced pulse broadening at the optical wavelength of 785 nm. In the following section we discuss the fabrication procedure for the pedestal waveguides. In section three we describe the techniques used for the measurement of the nonlinear refractive index of tantalum oxide and waveguide losses. In section four the experimental results are presented and discussed along with the future perspective for this platform.

2. Pedestal waveguide fabrication

The fabrication of Ta_2O_5 waveguides was done using pedestal waveguides since this process allows for significantly smaller propagation losses, and it is well suited for materials for which standard etching processes are not well established [12,15,16]. The process is illustrated in Fig. 1 and it was done on p-type silicon wafers. After standard cleaning, a dry oxide growth process is performed inside a furnace at 1135 °C for 1 hour, in a H_2 and O_2 gaseous mixture, obtaining a thermal silicon dioxide (SiO_2) with 150 nm thickness (blue layer in Fig. 1(a)). Subsequently, a photolithography process is performed to define the waveguide geometry (Fig. 1(a)). After developing the photoresist, the oxide is wet etched (Fig. 1(b)) using buffered oxide etch (BOE) for 2 minutes.

Figure 1(c) illustrates the isotropic etch of the silicon underneath the photoresist and the silicon dioxide layers. This is achieved with SF_6 plasma (26 sccm flow), with 100 W of RF power and 68 mTorr of pressure, for 3.5 minutes, leading to an etched structure 3.7 μm deep. The photoresist stayed undamaged during the etch, protecting the SiO_2 layer. Figure 1(c) shows how the silicon underneath the thin silica layers is undercut, leaving a silica 'hat' which allows a controlled deposition of the devices' core, protecting the sidewalls of the pedestal. In addition, this shape isolates the waveguide from the lateral slab waveguides, avoiding coupling losses.

The subsequent step is a wet oxidation process at 1150 °C performed on the silicon wafer, creating a thick SiO_2 layer (1.65 μm) underneath the silica 'hat' and in the lateral regions of the

Optics EXPRESS

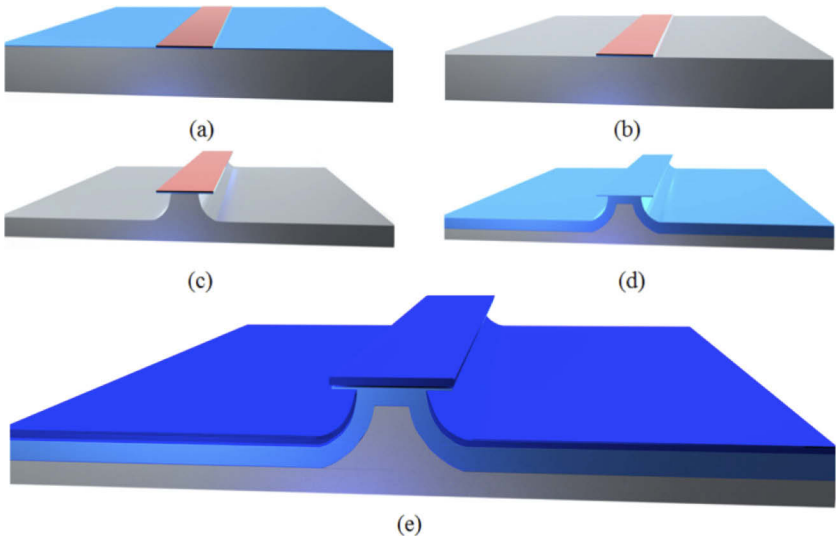

Fig. 1. Fabrication process of pedestal waveguides: (a) SiO_2 desposition and optical contact lithography; (b) Wet etch of SiO_2 layer; (c) Isotropic reactive ion etching of the silicon substrate; (d) Thermal oxidation; (e) Depostion of the Ta_2O_5 core.

pedestal structure (Fig. 1(d)). This oxide is in fact the lower cladding of the waveguides whereas the upper cladding is air. The refractive index of the thermally grown SiO_2 was measured using ellipsometry technique, and its value is 1.46. For this reason, the material used as a core must have a higher index to allow for total internal reflection (TIR) to take place inside the waveguide. The measured refractive index of Ta_2O_5 is 2.07. The core is deposited using the DC reactive sputtering technique (dark blue layer in Fig. 1(e)). The core is a 430 nm-thick layer of Ta_2O_5. The DC voltage used in the deposition process is 1.77 kV and the total process time is 50 min.

3. Nonlinear index and loss measurements methods

Pedestal waveguides with a total length of 3 cm were used for the propagation loss measurement, which was done using the top view technique. This technique consists on the acquisition of images with a CCD camera adapted to a microscope with 10× magnification to capture light scattered by the waveguides. The light scattered from the top surface of the waveguides is proportional to the intensity of light guided inside the core. This relation is a way to calculate propagation losses [17]. With digital treatment of the captured images, it is possible to obtain the intensity of the scattered light as a function of the distance along the propagation direction, which can be fitted using linear regression in order to obtain the slope and calculate the propagation losses.

In order to use Ta_2O_5 as a nonlinear platform based on the pedestal process, it is important to have low propagation losses as well as as a high nonlinear refractive index. The determination of n_2 was done using pulse spectral broadening measurements based on self-phase modulation (SPM) [13,14], considering that the broadening for a given power P_0 is related to the n_2 by [18]:

$$\frac{\omega_{max}}{\Delta\omega_0} = \frac{0.86 L_{eff} n_2 P_0 \omega_0}{c A_{eff}}, \tag{1}$$

where $\Delta\omega_0$ is the original spectral width (FWHM) of the pulse, ω_{max} is the spectral width after broadening due to SPM, P_0 is the peak power, ω_0 is the center angular frequency, c is the speed of light in vacuum, A_{eff} is the effective area calculated numerically using the finite element method

Optics EXPRESS

(FEM) and the effective length (L_{eff}) is given by:

$$L_{eff} = \frac{1 - e^{-\alpha d}}{\alpha}. \tag{2}$$

In this last equation α is the attenuation constant and d is the length of the waveguide.

4. Results and discussion

A scanning electron microscope (SEM) micrograph of the cross-section of a pedestal waveguide with Ta_2O_5 core is shown in Fig. 2(a). This waveguide has a 5 μm-wide, 430 nm-thick core. The thickness of the lower cladding silica layer is 1.65 μm and the height of the pedestal is approximately 3.6 μm. Since the refractive index of tantalum oxide (n = 2.07) is much larger than that of the silica lower cladding and air upper cladding, the mode is confined mostly in the core, as can be seen in Fig. 2(b), which shows the magnitude of the electric field's x component associated with the fundamental mode of a 5 μm-wide pedestal waveguide, obtained by FEM mode analysis. By inspection of Fig. 2(a), it is also possible to conclude that the core is well isolated from the silicon layer and the tantalum oxide slab waveguide formed on either side of the pedestal. This isolation is provided by the 'hat'-shaped structure formed by the core, which prevents Ta_2O_5 from being deposited on the region immediately underneath it. All of these factors contribute to low leakage losses.

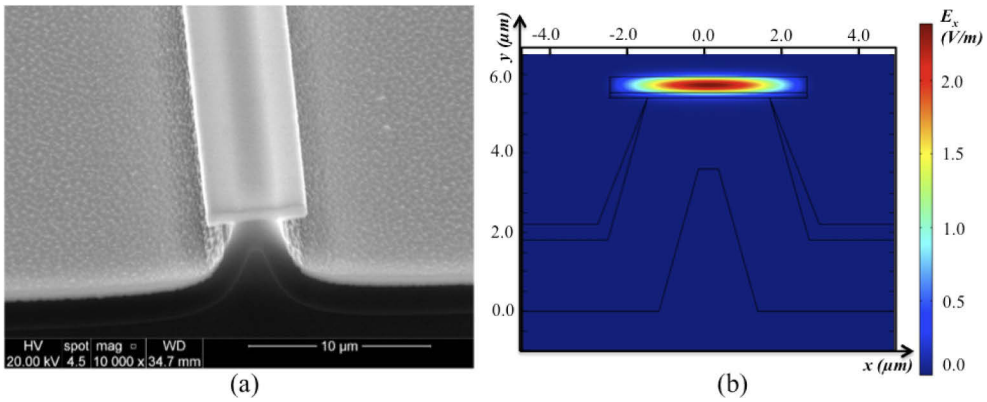

Fig. 2. (a) SEM micrograph of a 5 μm-wide pedestal waveguide. (b) Magnitude of the E-field's x component associated with the fundamental mode of a 5 μm-wide pedestal waveguide, obtained by FEM mode analysis.

The losses of the pedestal waveguides were measured via the top-view technique described in the previous section for waveguides with widths ranging from 5 μm to 100 μm. The measured propagation losses are plotted in Fig. 3(a) as a function of waveguide width. The minimum propagation loss corresponding to the 100 μm-wide waveguide is 0.1 dB·cm^{-1}. Note that all of the propagation losses measured are below 1.6 dB·cm^{-1}. These small losses are attributed to the modified pedestal process [12,16]. In fact, these values are significantly smaller than loss values presented in other works for tantalum oxide strip waveguides that are fabricated with conventional processes (e.g., 2.4 dB·cm^{-1} measured in [13]). The use of pedestals is a good alternative for reducing these losses. This is an important feature of the platform proposed in this work.

Figure 3(b) shows the spectra measured with an optical spectrum analyzer (OSA-USB2000+, from Ocean Optics) at the output of a 1.5 cm-long 80 μm-wide waveguide for different waveguide peak powers, ranging from 0.79 kW to 1.77 kW. For this experiment, we used 23 fs pulses generated by a Ti:sapphire amplified laser system (Femtopower Compact Pro HR/HP from

Optics EXPRESS

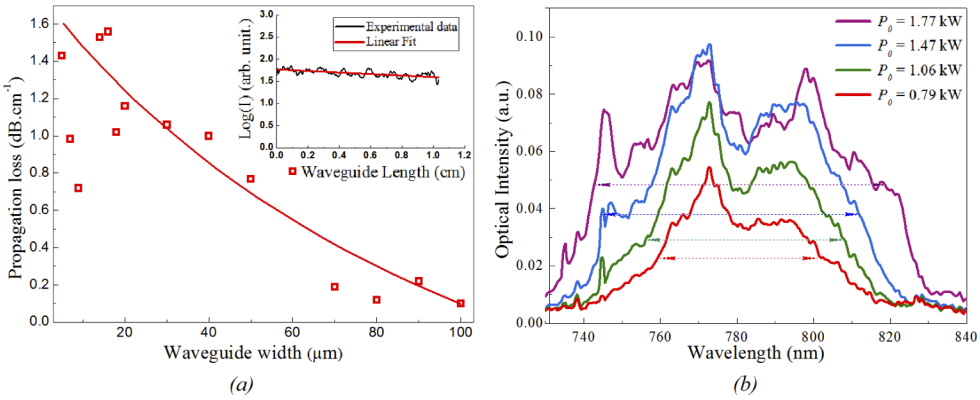

Fig. 3. (a) Propagation loss results of Ta_2O_5 pedestal waveguides in the 5 -100 μm width range. The inset shows the slope of the measured light intensity captured by the CCD camera as a function of the optical waveguide length. (b) Optical intensity spectra at the output of the waveguides for different peak powers inside the waveguide.

Femtolasers), centered at 785 nm, with 40 nm of bandwidth (FWHM), in a 4 kHz repetition rate train of pulses.

The pulses energy was attenuated by a series of neutral density filters, and their peak power was finely controlled using a half-wave plate and a polarizer in the optical path of the laser beam before it reached the waveguide. The polarizer was configured to transmit the horizontal polarization and the wave plate was used to control the power injected into the waveguide. A 10× objective was used to couple light into the integrated waveguides. The light at the waveguide's output was collected by an optical fiber leading to the optical spectrum analyzer.

The pulse spectral widths shown in Fig. 3(b) were used in Eq. (1) in order to calculate the effective n_2 of the structure. This nonlinear index does not correspond to that of tantalum oxide because part of the modal field of the pedestal waveguide permeates the air and the silica lower cladding. We have used mode analysis based on the finite element method (FEM) to find the fraction of the light intensity in each part of the waveguide. In conjunction with the known n_2 of silica as well as the effective n_2 obtained for the structure, this allowed us to obtain the nonlinear index of the core material Ta_2O_5. The effective or overall n_2 was considered to be equal to the average of the nonlinear indexes of the different regions of the waveguide (silica and air claddings and Ta_2O_5 core) weighed by the fraction of power in each region.

A nonlinear index value of $(5.8 \pm 2.0) \times 10^{-19} m^2W^{-1}$ was obtained for Ta_2O_5. This value is very close to n_2 values reported in the literature and is more than one order of magnitude larger than that of silica, which in conjunction with the low propagation losses makes pedestal Ta_2O_5 a great platform for nonlinear optical applications such as supercontinuum generation, frequency comb generation, wavelength conversion and parametric amplification. The presented n_2 value is the average of the n_2 values measured for waveguides with widths ranging from 7 μm to 100 μm. It is important to mention that the narrower waveguides support only a few modes, which means that they could be used for most of the nonlinear applications mentioned above.

5. Conclusion

We proposed, fabricated and analyzed a novel pedestal NLO platform based on Sputtered tantalum oxide, having measured its effective nonlinear refractive index. The value obtained for the n_2 of Ta_2O_5 is $(5.8 \pm 2.0) \times 10^{-19}$ m^2W^{-1}, which is more than one order of magnitude greater than that of silicon dioxide. The propagation losses obtained for Ta_2O_5 pedestal waveguides are as low as 0.1 dB·cm^{-1}, and smaller than 1.6 dB·cm^{-1} in all cases. These losses are smaller than

Optics EXPRESS

the ones reported in the literature, which makes this platform of great interest to make low loss resonators with large quality factors, essential for NLO applications such as frequency comb generation. The low propagation losses were obtained in spite of the fact that optical contact lithography was used, and can be improved even further if electron beam lithography is used, as is done in many of the related works where Ta_2O_5 strip waveguides have been demonstrated. For these reasons, we believe the tantalum oxide pedestal platform to be a promising candidate for integrated nonlinear optics devices.

Funding

Conselho Nacional de Desenvolvimento Científico e Tecnológico (305447/2017-3, 32088/2018-0); Fundação de Amparo à Pesquisa do Estado de São Paulo.

Disclosures

The authors declare no conflicts of interest.

References

1. D. Yelin, D. Oron, S. Thiberge, E. Moses, and Y. Silberberg, "Integrated nonlinear optical signal processing in cmos compatible platforms," Opt. Express **11**(12), 1385–1391 (2003).
2. Y. Okawachi, A. Gaeta, and M. Lipson, "Breakthroughs in nonlinear silicon photonics 2011," IEEE Photonics J. **4**(2), 601–606 (2012).
3. J. Leuthold, C. Koos, and W. Freude, "Nonlinear silicon photonics," Nat. Photonics **4**(8), 535–544 (2010).
4. A. Griffith, R. Lau, J. C. Y. Okawachi, A. Mohanty, R. Fain, Y. Lee, C. P. M. Yu, C. P. A. Gaeta, and M. Lipson, "Silicon-chip mid-infrared frequency comb generation," Nat. Commun. **6**(1), 6299 (2015).
5. L. Xu, N. Ophir, M. Menard, R. K. W. Lau, A. C. Turner-Foster, M. A. Foster, M. Lipson, A. L. Gaeta, and K. Bergman, "Simultaneous wavelength conversion of ask and dpsk signals based on four-wave-mixing in dispersion engineered silicon waveguides," Opt. Express **19**(13), 12172–179 (2011).
6. N. Ophir, J. Chan, K. Padmaraju, A. Biberman, A. C. Foster, M. A. Foster, M. Lipson, A. L. Gaeta, and K. Bergman, "Continuous wavelength conversion of 40-gb/s data over 100 nm using a dispersion-engineered silicon waveguide," IEEE Photonics Technol. Lett. **23**(2), 73–75 (2011).
7. J. S. Levy, K. Saha, Y. Okawachi, M. A. Foster, A. L. Gaeta, and M. Lipson, "High-performance silicon-nitride-based multiple-wavelength source," IEEE Photonics Technol. Lett. **24**(16), 1375–1377 (2012).
8. A. Pasquazi, Y. Park, J. Azana, F. Légaré, R. Morandotti, B. E. Little, S. T. Chu, and D. J. Moss, "Efficient wavelength conversion and net parametric gain via four wave mixing in a high index doped silica waveguide," Opt. Express **18**(8), 7634–7641 (2010).
9. Y. Okawachi, K. L. M. Yu, D. O. Carvalho, S. Ramelow, A. Farsi, M. Lipson, and A. L. Gaeta, "Dual-pumped degenerate kerr oscillator in a silicon nitride microresonator," Opt. Lett. **40**(22), 5267–5270 (2015).
10. K. Ooi, D. Ng, T. Wang, A. Chee, S. Ng, Q. Wang, L. Ang, A. Agarwal, L. Kimerling, and D. Tan, "Pushing the limits of CMOS optical parametric amplifiers with usrn: Si_7N_3 above the two-photon absorption edge," Nat. Commun. **8**(1), 13878–10 (2017).
11. L. Razzari, D. Duchesne, M. Ferrera, R. Morandotti, S. Chu, B. Little, and D. Moss, "CMOS-compatible integrated optical hyper-parametric oscillator," Nat. Photonics **4**(1), 41–45 (2010).
12. E. G. Melo, M. I. Alayo, and D. O. Carvalho, "Study of the pedestal process for reducing sidewall scattering in photonic waveguides," Opt. Express **25**(9), 9755–9760 (2017).
13. Y.-Y. Lin, C.-L. Wu, W.-C. Chi, Y.-J. Chiu, Y.-J. Hung, A.-K. Chu, and C.-K. Lee, "Self-phase modulation in highly confined submicron Ta_2O_5 channel waveguides," Opt. Express **24**(19), 21633–21641 (2016).
14. C.-Y. Tai, J. S. Wilkinson, N. M. B. Perney, M. C. Netti, F. Cattaneo, C. E. Finlayson, and J. J. Baumberg, "Determination of nonlinear refractive index in a Ta_2O_5 rib waveguide using self-phase modulation," Opt. Express **12**(21), 5110–5116 (2004).
15. D. O. Carvalho, L. R. Kassab, V. D. del Cacho, D. M. da Silva, and M. I. Alayo, "A review on pedestal waveguides for low loss optical guiding, optical amplifiers and nonlinear optics applications," J. Lumin. **203**, 135–144 (2018).
16. F. A. Bonfim, R. C. Rangel, D. M. da Silva, D. O. Carvalho, E. G. Melo, M. I. Alayo, and L. R. Kassab, "A new fabrication process of pedestal waveguides based on metal dielectric composites of Yb^{3+}/Er^{3+} codoped PbO-GeO_2 thin films with gold nanoparticles," Opt. Mater. **86**, 433–440 (2018).
17. Y. Okamura, S. Yoshinaka, and S. Yamamoto, "Measuring mode propagation losses of integrated optical waveguides: a simple method," Appl. Opt. **22**(23), 3892–3894 (1983).
18. G. P. Agrawal, *Nonlinear Fiber Optics* (Academic Press, 2013).